Ocean Engineering 218 (2020) 108126

Contents lists available at ScienceDirect

Ocean Engineering

journal homepage: www.elsevier.com/locate/oceaneng

Controlled course-keeping simulations of a ship under external disturbances

G. Budak *, S. Beji

Faculty of Naval Architecture and Ocean Engineering, Istanbul Technical University, Maslak, 34469, Istanbul, Turkey

ARTICLE INFO

Keywords:
Ship manoeuvring
Ship control under disturbances
PD controller
Fuzzy controller

ABSTRACT

A Simulink code for numerical simulation of ship manoeuvring is developed based on the appropriate differential equations. Both the Abkowitz and MMG models are implemented as choices according to the available hydrodynamic particulars of a given ship. Reliability of the developed code is assessed by performing the turning and zigzag tests for two different ships, employing the Abkowitz and MMG models in turn according to the available characteristics. As a field study, real time records of the routes followed by a passenger ship crossing the Strait of Istanbul under the disturbing effect of a lateral current were made. One of the vessels tested was autopiloted by a classic PD and a fuzzy-like PD controller separately, guiding the ship to a target destination under cross-current as in the Strait of Istanbul. Performances of these controllers in comparison with the human piloting of the field observations reveal that under disturbing current effects both controllers provide relatively shorter travel paths and the fuzzy-like PD controller stands as a better choice between the two.

1. Introduction

Temporary variations of a sea state impose time-dependent disturbing forces to a sea-going vessel and consequently necessitate appropriate corrections to steer the vessel to a desired location while continuously monitoring external conditions. With the advent of various branches of engineering, customarily human piloting of a vessel has been advancing towards auto-piloting. Likewise, if a vessel is required to remain at a certain point the actions taken are considered as dynamic positioning. Both tasks of piloting and positioning fall into the realm of ship manoeuvring, which in turn implies a set of time-dependent differential equations with definite controllable terms representing steering forces and moments. Thus, the entire problem may be viewed as composed of two main parts; first, solving the differential equations governing ship manoeuvring and second, determining the appropriate commands to the control terms. All these, of course, are performed in a coupled manner by taking into account responses of the vessel as feedback.

Since the early 1960's ship manoeuvring has been among intensely studies areas of naval architecture. Reasons for devoting such considerable efforts to the subject may be attributed to a variety of parameters involved in modelling the ship manoeuvring. To begin with, hydrodynamic behaviour of a ship in motion depends closely on her particular form and this dependency must be formulated for different motions. Determination of external forces due to waves and currents for a varying sea state poses another challenge; moreover, there are the wind forces acting on the superstructure. It is therefore not surprising that an enormous literature has been accumulated in these and related subjects as presented in a relatively recent review in (Hirdaris et al., 2014).

Increasing computational capabilities have led to more detailed investigations by numerical means. A Simulink-based marine control system was described in detail by Perez et al. (2006). Moreira, Fossen and Soares (Moreira et al., 2007) presented a path following control system for a surface vessel with particular reference to a possible future application to *Esso Osaka* tanker. Seo and Kim (2011) simulated coupled ship manoeuvring and motions in presence of waves. Slow-steaming performance of a ship in waves was considered in Tezdoğan et al. (Tezdogan et al., 2015) with the aim of reducing operational costs. In a study concerning ship optimization (Tahara et al., 2006) manoeuvrability performance was included among multiple objectives of the optimization process. Kim et al. (2017) investigated the added resistance of KVLCC2 ship in head seas for various speeds and wave conditions. Kurowski, Köckritz and Korte (Kurowski et al., 2013) presented a comprehensive manoeuvring planning system for marine vessels. Travel

* Corresponding author.
E-mail addresses: budakg@itu.edu.tr (G. Budak), sbeji@itu.edu.tr (S. Beji).
URL: http://eng.serdarbeji.com (S. Beji).

https://doi.org/10.1016/j.oceaneng.2020.108126
Received 1 May 2020; Received in revised form 10 August 2020; Accepted 16 September 2020
Available online 9 October 2020

Nomenclature

β_c	Current angle measured due north	L_{oa}	Overall length of ship
δ	Rudder angle	m	Mass of ship
γ_{rc}	Relative current angle between heading angle and current angle	N	Hydrodynamic moment
Ψ	Heading angle of ship	n	Propeller revolution per second
ψ_d	desired heading angle	$r = \dot{\psi}$	Angular velocity of the ship or 'yaw rate'
ρ	Seawater density	t_R	Steering resistance deduction factor
a_H	Rudder force increase factor	U	Cruising speed
A_R	Profile area of movable part of mariner rudder	u, v	Surge and lateral velocity at the centre of gravity, respectively
A_{Fc}	Frontal projected area of the ship exposed to the current	U_A	Advance velocity
A_{Lc}	Lateral projected area of the ship exposed to the current	w	Wake coefficient
D	Propeller diameter	X, Y	Longitudinal and transverse hydrodynamic forces acting on the ship
F_N	Rudder normal force	x_G	Horizontal distance between origin O and centre of gravity of the ship
I_{zz}	Moment of inertia with respect to z-axis	x_H	Longitudinal coordinate of acting point of additional lateral force due to propeller-hull interaction
J	Advance coefficient	x_R	Longitudinal coordinate of rudder position($= -0.5L_{pp}$)
k_0, k_1, k_2	Polynomial coefficients defining K_T		

duration and fuel consumption were used to determine the optimum route of a vessel by Fang and Lin (2015) for efficiency and economy.

As early as 1977 Källström et al. (1977) suggested two adaptive autopilots, simple and advanced, to reduce the fuel consumption of tankers. Çimen and Banks (Cimen and Banks, 2004) developed optimal tracking controllers for non-linear systems and applied these on the ESSO oil tanker, claiming better efficiency compared to manual open-loop operation. Relatively recently, Bhattacharya et al. (2011) proposed a fuzzy autopilot control for ship manoeuvring in the absence of external forces.

The present work introduces a Simulink code for ship manoeuvring simulations with choices of the Abkowitz and MMG models. Inclusion of two different methods, a novelty of the present work, makes the code a versatile tool that can be switched to either model, depending on the available hydrodynamic characteristics of the ship. In order to test the proper working of each model the benchmark tests are done by considering two vessels with parameters suitable for the Abkowitz and MMG models, respectively.

Another novelty of the present simulator is the integration of a controller for determining a possible optimum route for a vessel moving to a target destination under the influence of disturbing forces. As an additional aspect, two different controllers; namely, PD and fuzzy-like PD are used and their performances are compared. Passenger boats crossing the Strait of Istanbul are taken as the basis of these simulations. Six different cases involving travel of a vessels between two locations under cross-currents are autopiloted by a classical PD and a fuzzy-like PD controllers separately for three different current speeds. Routes dictated by these controllers are compared to those of human steered passenger boat, which were recorded during a field study. Comparisons favour the performance of the fuzzy-like PD controller due to its relatively shorter paths and accuracy of targeting the destination.

2. Governing equations of ship manoeuvring and assumptions

Differential equations governing ship manoeuvring are consist of force and moment expressions representing surge, sway, and yaw motions in the horizontal plane with no roll, pitch, and heave. Thus, while the complete motions of a ship have 6 degrees of freedom (dof), the manoeuvring equations have 3 dof.

Euler's equations of motion expressed in terms of coordinates fixed to the origin O at the mid-length of moving vehicle whose motion is restricted to horizontal (x,y) plane as shown in Fig. 1, are given by [6, p.467]

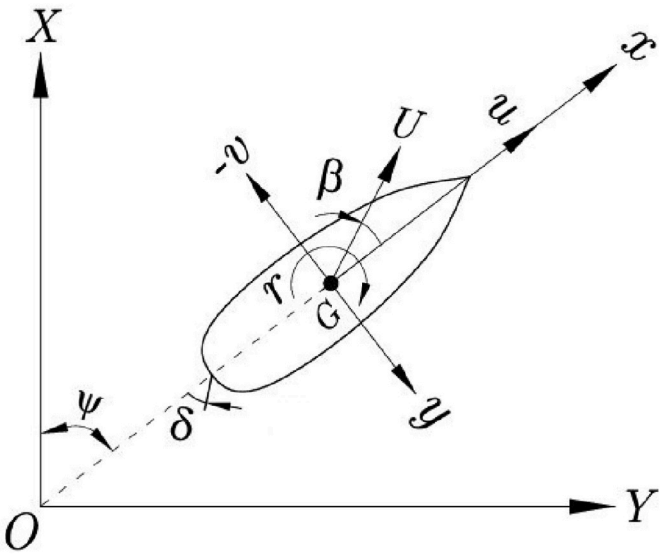

Fig. 1. Orientation of fixed and moving co-ordinates.

$$\begin{aligned} m(\dot{u} - vr - x_G r^2) &= X(u, v, r, \dot{u}, \dot{v}, \dot{r}, \delta) \\ m(\dot{v} + ur + x_G \dot{r}) &= Y(u, v, r, \dot{u}, \dot{v}, \dot{r}, \delta) \\ I_{zz}\ddot{\psi} + mx_G(\dot{v} + ur) &= N(u, v, r, \dot{u}, \dot{v}, \dot{r}, \delta) \end{aligned} \tag{1}$$

where u and v are the instantaneous velocities respectively in the $x-$ and $y-$ directions, m the mass of the ship, I_{zz} the mass moment of inertia with respect to the vertical axis at the centre of gravity of the ship, X, Y the longitudinal and transverse hydrodynamic forces acting on the ship, N the hydrodynamic moment, $r = \dot{\psi}$ the angular velocity of the ship or the "yawing rate", δ the rudder angle, and x_G the horizontal distance between the origin O and the centre of gravity of the ship. Overdot denotes differentiation with respect to time.

The usual assumptions of manoeuvring and course-keeping modelling are made. Specifically, the ship is taken as a rigid body with port-starboard symmetry, the lateral velocity of the ship is regarded small compared to the cruising speed while the metacentric height is large enough to ensure the ship's stability. Hydrodynamics forces acting on the ship are treated as quasi-steady, the effects of rolling, pitching, and heaving on manoeuvring are neglected, and wave-making effects are

ignored completely. In turning and zigzag tests no external forces at all are applied other than the appropriate rudder force. Course-keeping simulations of a boat crossing the Bosphorus on the other hand are performed under two different controllers while the ship is subject to a lateral current force and turning moment proportional to the current speed. Any other external disturbance such as wave and wind forces and moments acting on the ship can be implemented in exactly the same manner. Finally, numerical solutions of the governing equations both for the Abkowitz and MMG model are accomplished in a coupled manner by the default integrator of the Simulink.

2.1. Abkowitz Model

Basically there are two approaches of expressing the hydrodynamic forces acting on a ship. The older one is the Abkowitz method which expresses X, Y, and N as Taylor series. The relatively recent and currently preferred one is the Manoeuvring Modelling Group model or briefly the MMG approach which decomposes the forces and moment into several sub-components and expresses especially the propeller and rudder forces by semi-empirical formulas. In this work the programming is done to comprise both methods so that the user can select the appropriate model for the purposes. For instance, if all the hydrodynamic derivatives are available from experiments or by some other means, as in §3, the Abkowitz method may be preferred. On the other hand, if only the main characteristics of the ship are available the MMG method with empirical expressions for each force component is a better choice.

For the Abkowitz method or the so-called whole ship method the present algorithm uses the following third-order Taylor series expansions for the total hydrodynamic forces and moment [6, p.680].

$$\begin{aligned}&\left(m-X_{\dot u}\right)\dot u = X\\ &\left(m-Y_{\dot v}\right)\dot v + \left(mx_G - Y_{\dot r}\right)\dot r = Y\\ &\left(N_{\dot v}+mx_G\right)\dot v + \left(I_{zz}-N_{\dot r}\right)\dot r = N\end{aligned} \tag{2}$$

The right-hand side of equation (2) can be written as

$$\begin{aligned}X &= X(0) + X_u\Delta u + \tfrac{1}{6}X_{uuu}u^3\\ &+\tfrac{1}{2}\left(X_{uu}u^2 + X_{vv}v^2 + X_{\delta\delta}\delta^2 + X_{v\delta}v\delta\right) + X_C\\ Y &= Y(0) + Y_\delta\delta + Y_v v + (Y_r - mU)r\\ &+\frac{1}{6}\left(Y_{vvv}v^3 + Y_{\delta\delta\delta}\delta^3\right)\\ &+\frac{1}{2}\left(Y_{vvr}v^2r + Y_{vv\delta}v^2\delta + Y_{\delta\delta v}\delta^2 v\right) + Y_C\\ N &= N(0) + N_\delta\delta + N_v v + (N_r - mx_G U)r\\ &\underset{+\frac{1}{6}\left(N_{vvv}v^3+N_{\delta\delta\delta}\delta^3\right)}{}\\ &\underset{+\frac{1}{2}\left(N_{vvr}v^2r+N_{vv\delta}v^2\delta+N_{\delta\delta v}\delta^2 v\right)+N_C}{}\end{aligned} \tag{3}$$

where $X(0)$ is the force in the $x-$ direction at the equilibrium condition when the ship is moving at the steady cruising speed U. In other words, $X(0)$ represents the total ship resistance at the speed U in the longitudinal direction. $\Delta u = u - U$ is the relatively small variation of instantaneous ship speed u from the cruising speed U, and $X_{\dot u}$ is the so-called added-mass in the $x-$ direction, arising from the acceleration or deceleration $\dot u$ of the ship. Detailed explanations concerning the remaining terms may be found in Comstock, 1986.

2.2. MMG model

The MMG model was developed by Japanese researchers hence most material on this model is in Japanese. The earliest contribution in English may be attributed to Ogawa and Kasai (1978) while relatively recent ones are Yoshimura (2005), and Yasukawa and Yoshimura (2015). Many researchers working in the field have been preferring the MMG model; for practical reasons it is more popular (Aksu and Köse, 2017; Sukas et al., 2019a; Xia et al., 2018).

Equations of manoeuvring motions according to the MMG model are expressed as

$$\begin{aligned}&\left(m+m_x\right)\dot u - \left(m+m_y\right)vr - mx_G r^2 = X\\ &\left(m+m_y\right)\dot v + \left(m+m_x\right)ur + mx_G\dot r = Y\\ &\left(I_{zz}+mx_G^2+J_{zz}\right)\dot r + mx_G(\dot v + ur) = N\end{aligned} \tag{4}$$

where m_x and m_y denote respectively the added masses in the $x-$ and $y-$ directions, and J_{zz} stands for the added mass moment of inertia.

The MMG approach separates the total force components and moment into different modules. Typically, three components which are associated with the ship hull, propeller, and rudder are considered. In this work additionally the external forces and moment due to currents are included as the algorithm developed aims at autopiloting a ship under disturbing forces. Denoting these components by the subscripts H, P, R, and C, respectively the total forces and moment are decomposed as,

$$\begin{aligned}X &= X_H + X_P + X_R + X_C\\ &\underset{N=N_H+N_P+N_R+N_C}{Y=Y_H+Y_P+Y_R+Y_C}\end{aligned} \tag{5}$$

Hydrodynamic forces X_H and Y_H and moment N_H acting on the ship hull may be expressed as,

$$\begin{aligned}X_H &= -R_0 + X_{vv}v^2 + X_{vr}vr + X_{rr}r^2 + X_{vvvv}v^4\\ Y_H &= Y_v v + Y_r r + Y_{vvv}v^3\\ &+Y_{vvr}v^2r + Y_{vrr}vr^2 + Y_{rrr}r^3\\ N_H &= N_v v + N_r r + N_{vvv}v^3\\ &+N_{vvr}v^2r + N_{vrr}vr^2 + N_{rrr}r^3\end{aligned} \tag{6}$$

where R_0 is the ship resistance force at constant cruising speed U in the $x-$ direction. Note that the lateral hull force and moment are taken to the third-order, which is reported to perform better compared to the second-order (Aksu and Köse, 2017; Yasukawa and Yoshimura, 2015).

$$\begin{aligned}X_P &= (1-t)\,T\\ &\underset{N_P=0}{Y_P=0}\end{aligned} \tag{7}$$

where T is the propeller thrust and t the thrust reduction coefficient. The trust T is related to the thrust coefficient K_T by the relationship

$$T = \rho n^2 D^4 K_T(J) \tag{8}$$

in which ρ is the seawater density, n the propeller revolution per second, D the propeller diameter, and J the advance coefficient. The thrust coefficient K_T may be approximated by a second-degree polynomial in J so that $K_T(J) = k_0 + k_1 J + k_2 J^2$ with k_0, k_1, and k_2 being the constants characterizing the propeller. Recalling that the advance coefficient J is defined as $J = V_A/nD$ and that the advance velocity V_A is related to the ship speed V by $V_A = V(1-w)$, w being the wake coefficient, give for the advance coefficient corresponding to the instantaneous ship speed u as $J = u(1-w)/nD$. Depending on the ship characteristics the wake coefficient w is determined from appropriate empirical formulas. Also, the wake coefficient for a ship advancing in a straight course is different from the wake coefficient corresponding to a ship in manoeuvring and they are related by empirical relations.

Effective rudder forces and moment X_R, Y_R, N_R are given by

$$\begin{aligned}X_R &= -(1-t_R)F_N\sin\delta\\ &\underset{N_R=-(x_R+a_H x_H)F_N\cos\delta}{Y_R=-(1+a_H)F_N\cos\delta}\end{aligned} \tag{9}$$

where δ is the rudder angle as indicated before, t_R and a_H the coefficients representing interactions between rudder and hull, $x_R = -0.5L_{pp}$ the distance between amidship and the lateral force applied by the rudder, x_H the longitudinal coordinate of acting point of the additional lateral force due to propeller-hull interaction. The rudder normal force F_N is given by

$$F_N = \frac{1}{2}\rho A_R U_R^2 f_\alpha \sin\alpha_R \tag{10}$$

in which A_R is the rudder area, $U_R = \sqrt{u_R^2 + v_R^2}$ the inflow velocity to the rudder with u_R and v_R being the longitudinal and lateral inflow velocity components, and $\alpha_R = \delta - \arctan(v_R/u_R)$ the effective inflow angle. u_R and v_R can be determined with the aid of appropriate empirical relationships [30, p.41–42].

Hydrodynamic forces and moment acting on a ship due to a current flowing at an angle may be expressed as [9, p.155]

$$\begin{array}{l} X_C = \frac{1}{2}\rho A_{Fc} C_X(\gamma_{rc})\,|u_c|u_c \\ Y_C = \frac{1}{2}\rho A_{Lc} C_Y(\gamma_{rc})\,|v_c|v_c \\ N_C = \frac{1}{2}\rho A_{Lc} L_{oa} C_N(\gamma_{rc})\,|v_c|v_c \end{array} \tag{11}$$

where ρ is the density of seawater, L_{oa} is the length overall, A_{Fc} and A_{Lc} are respectively the frontal and lateral projected areas of the ship exposed to the current. u_c and v_c the components of current velocity V_c on x-axes and y-axes, the angle γ_{rc}, and the component velocities are given by

$$u_c = -V_c\cos\gamma_c, \quad v_c = V_c\sin\gamma_c, \quad \gamma_{rc} = \beta_c - \psi \tag{12}$$

where $V_c = \sqrt{u_c^2 + v_c^2}$ is the current velocity, β_c the direction of the ocean current, and ψ the heading angle, which is used in updating the current force coefficients at every time step. It is possible to express the current coefficients $C_X(\gamma_{rc})$, $C_Y(\gamma_{rc})$, and $C_N(\gamma_{rc})$ as polynomials in γ_{rc} by establishing best fit to the curves given in Fig. 2 [9, p.154]. Note that these coefficients are strictly valid for a tanker but may provide acceptable values for other ship types.

3. Numerical solutions of manoeuvring equations for benchmark tests

Depending on the availability of parameters, the Abkowitz model, equations (2) and (3), or the MMG model, equations (4) and (5), is numerically solved using a Matlab-Simulink code, which is specifically developed for simulating the manoeuvres of a ship under external disturbances. The solution modules created in Simulink for the Abkowitz and MMG models are shown in Figs. 3 and 4, respectively.

In order to test the reliability and accuracy of the numerical solver, benchmark tests for two different vessels are carried out. The first test is the turning test for ±35° rudder angles for two separate runs. The second test is the zigzag manoeuvre performed by applying ±10° rudder angles alternately. Thus, two benchmark tests are simulated for two different vessels by employing the Abkowitz and MMG models separately to each vessel.

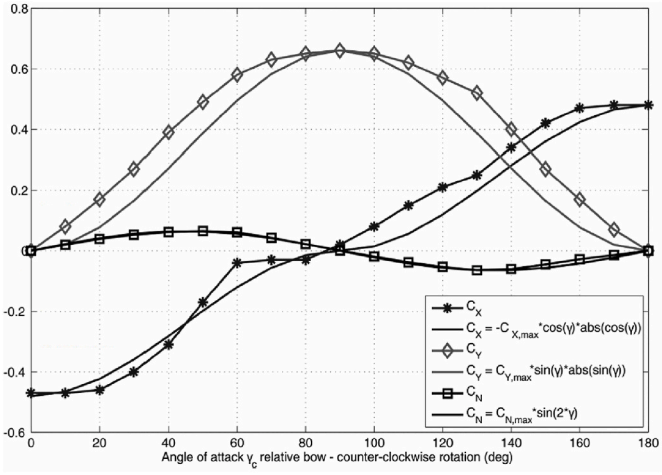

Fig. 2. Experimental current coefficients C_X, C_Y and C_N for a tanker. Notice that γ_c is taken counter clockwise direction and the angle of attack is zero, $\gamma_c = 0^o$, for a current in the bow (from Fossen (Fossen, 2011)).

$$\begin{array}{l} C_X(\gamma_{rc}) = -0.0665\gamma_{rc}^5 + 0.5228\gamma_{rc}^4 - 1.4365\gamma_{rc}^3 \\ \qquad +1.6024\gamma_{rc}^2 - 0.2967\gamma_{rc} - 0.4691 \\ C_Y(\gamma_{rc}) = 0.1273\gamma_{rc}^4 - 0.802\gamma_{rc}^3 + 1.3216\gamma_{rc}^2 \\ \qquad -0.1799\gamma_{rc} \\ C_N(\gamma_{rc}) = -0.014\gamma_{rc}^5 + 0.1131\gamma_{rc}^4 - 0.2757\gamma_{rc}^3 \\ \qquad +0.1617\gamma_{rc}^2 + 0.0728\gamma_{rc} \end{array} \tag{13}$$

3.1. Tests of a fishing vessel using Abkowitz model

The benchmark tests of a fishing vessel are done by the use of the Abkowitz model. The main characteristics and hydrodynamic coefficients of the fishing vessel *Città di Genova*, studied extensively by Obreja et al. (2010), are given in Tables 1 and 2, respectively. Note that the hydrodynamic coefficients include the propeller and rudder derivatives hence supply all the necessary quantities for running the Abkowitz model.

The non-dimensional coefficients presented in Table 2 are converted to dimensional coefficients by the use of conversion factors given in Table 3.

The graph of turning tests of the fishing vessel for ±35° rudder angles is displayed in Fig. 5. In accord with the nature of the Abkowitz model the turning circles are completely symmetric about the vertical axis. This symmetry is not observed in the turning tests simulated via the MMG model, which produces more realistic results by taking into account the effect of propeller rotation.

Table 4 presents the turning test parameters as computed by Obreja et al. (2010), the Tribon code, which was also presented in Obreja et al., 2010, and the present code. Overall the present work agrees well with Obreja et al. (2010) while the Tribon code differs appreciably from both of these. The only exception is the steady turning diameter for which the present code differs from the other two. To comment on the sources of differences is difficult; presumably all the programs use the same equations and the same hydrodynamics coefficients but the results are not the same. Nevertheless, some meaningful considerations can be put forward. The tactical and steady diameters of Obreja et al. (2010) are nearly the same and this does not sound quite reasonable. On the other hand, if a ratio is established between the tactical diameters of the present work and Tribon code, 3.03/3.93 = 0.77, the present work should have a steady diameter of 3.09·0.77 = 2.38, which is not much different from the computed value of 2.49. Such reasoning is meaningful as the Tribon code has consistently greater results compared to the present work.

The second benchmark test is the zigzag manoeuvre which is simulated by applying ±10° rudder angles alternately. The graph in Fig. 6 depicts the experimental measurement (black line) and the numerical simulation employing the Abkowitz method (red line). The rudder angle δ (blue line) is also drawn as a reference for determining the overshoot angles. Overall the simulation is in quite acceptable agreement with the measurement hence the reliability of the present code is established, especially when the results of turning test are also considered.

3.2. Tests of KVLCC2 tanker using MMG model

Tests parallel to the previous subsection are now carried out for the KVLCC2 tanker using the MMG model. The particulars and hydrodynamic coefficients of the KVLCC2 tanker as studied by Yasukawa and Yoshimura (2015), are given in Tables 5 and 6, respectively. For this case the MMG model is more suitable because the propeller and rudder coefficients are not provided and these parameters must be determined by empirical means.

The non-dimensional coefficients given in Table 6 are converted to

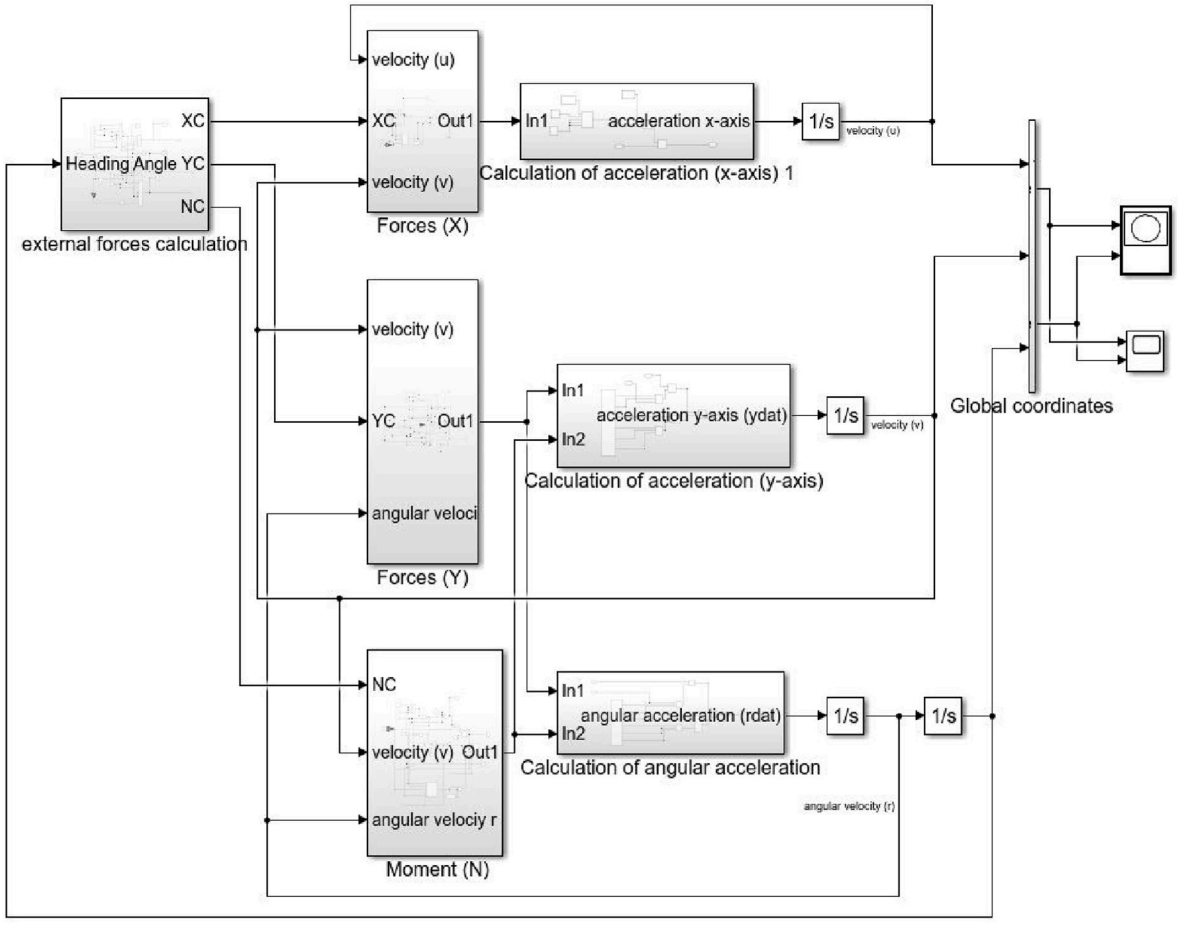

Fig. 3. Simulink module for Abkowitz Model.

dimensional coefficients by the use of conversion factors given in Table 7.

Turning tests of the KVLCC2 tanker for $\pm 35^{o}$ rudder angles are shown in Fig. 7. Note that the turning circles are not symmetric about the vertical axis. This asymmetry is typical for the turning tests simulated by employing the MMG model due to the difference in steering parameters which take into account the effect of propeller rotation.

Table 8 gives definite turning test parameters as computed by MARIN FR. (SIMMAN, 2008), Yasukawa and Yoshimura (2015), Sukas et al. (2019b), and the present code. While MARIN FR. and Sukas et al. (2019b) have a good overall agreement, the computations of the present work agree better with those of Yasukawa and Yoshimura (2015). As for the corresponding simulation of the fishing vessel it is not easy to determine the reason or reasons for two distinct grouping of results; nevertheless, a reasonable agreement among all computations is obvious.

As for the fishing vessel the zigzag manoeuvre for the KVLCC2 tanker is simulated by applying $\pm 10^{o}$ rudder angles alternately. Since no experimental or actual measurement is available for this vessel the simulation of Yasukawa and Yoshimura (2015) (black line) is plotted together with the present simulation (red line) in Fig. 8 for comparison. Quite similar to the good agreement observed for the turning test parameters the zigzag manoeuvre simulation of the present code agrees well with that of Yasukawa and Yoshimura (2015). After conducting these benchmark tests with two different methods for two different vessels with acceptable results it is probably safe to declare the present code reliable.

4. PD and fuzzy-like PD controllers

Recent technological achievements have made the controllers a very important part of industrial applications. A controller is basically a feedback mechanism which adjusts the control variable such that the error between the obtained and desired output is minimized. Currently, more than 90% of controllers are Proportional-Integral-Derivative (PID) controllers or varieties of PID controllers. Proportional (P) and Integral (I) modes alone can be used as single modes but the use of Derivative (D) mode alone is uncommon. Depending on the characteristics of application, Proportional-Integral (PI) and Proportional-Derivative (PD) combinations are most commonly used. PID-type controllers are preferred in wide range of application areas such as vehicle control, electronic appliances, etc. as they are simple, effective and reliable. A PID controller consists of three controls; namely, a proportional control $u(t) = K_P\, e(t)$, an integral control $u(t) = K_I \int_0^t e(\tau)d\tau$, and a derivative control $u(t) = K_D\, de(t)/dt$. Here, $u(t)$ is the control force (input) to the system, $e(t) = r(t) - y(t)$ is the error between the desired (reference) signal and actual (output) signal (Johnson and Moradi, 2005).

Performance of PID-type controllers can be enhanced by introducing a fuzzy-logic block for the decision making process. Fuzzy logic brings a definite artificial intelligence into the PID controller thus increasing the effectiveness of it. The performance of fuzzy-like PID controllers are better with self-tuning abilities and adaptation to uncertain, time-dependent non-linear systems (Feng and X-K., 2018; Le et al., 2004).

In the present work two controllers, a PD and a fuzzy-like PD, are separately incorporated into the Simulink code developed. The selected controller steers the ship by dictating the rudder angle while the Simulink manoeuvring code simultaneously computes the path of the

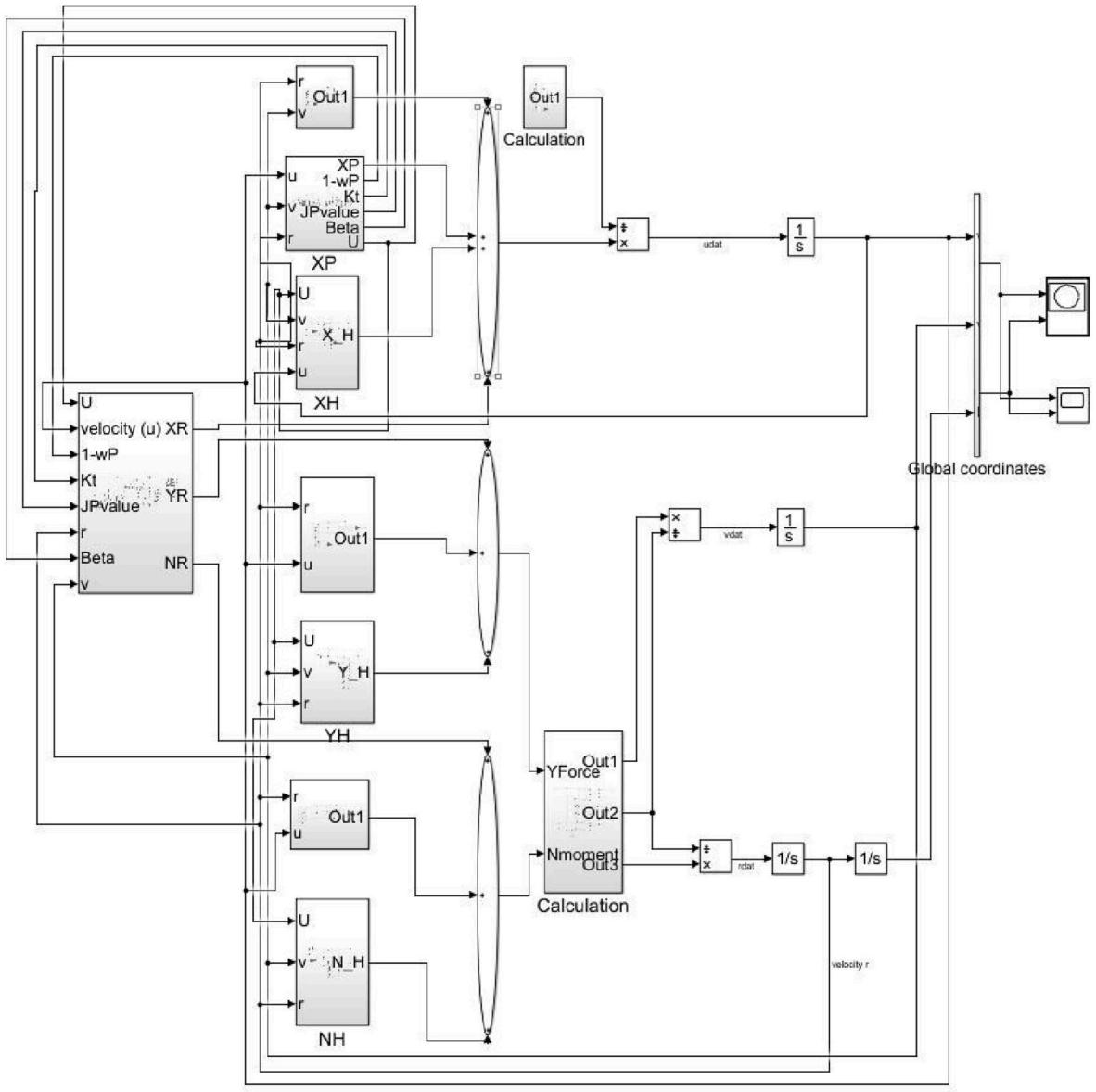

Fig. 4. Simulink module for MMG Model.

Table 1
Main characteristics of fishing vessel.

L_{OA}	32.7 m
L_{PP}	25.0 m
B	8.0 m
T	2.58 m
∇	296 m^3
C_B	0.574
k_{zz}	6.9 m
X_G	11.32 m
V	12.0 knots

ship. Thus, the route under external disturbances can be computed and the ship is guided to a desired terminal point by the controller. Like the manoeuvring code which uses two different methods, Abkowitz and MMG, the controller has two options, PD and fuzzy-like PD, for operating the vessel.

Table 2
Hydrodynamic coefficients of fishing vessel.

$\times 10^{-5}$	$\times 10^{-5}$	$\times 10^{-5}$
$X'_u = -189.3$	$Y'_v = -4539.4$	$N'_v = -1793.6$
$X'_{\dot{u}} = -2279.8$	$Y'_{\dot{v}} = -2998.0$	$N'_{\dot{v}} = 2757.6$
$X'_{uu} = -527.8$	$Y_r = 3326.7$	$N'_r = 1146.3$
$X'_{uuu} = -423.0$	$Y'_{\dot{r}} = 630.1$	$N'_{\dot{r}} = -211.1$
$X'_\delta = 225.3$	$Y'_\delta = 624.7$	$N'_\delta = -278.0$
$X'_{vv} = -919.0$	$Y'_{\delta\delta\delta} = -668.4$	$N'_{\delta\delta\delta} = 202.2$
$X'_{\delta\delta} = -371.0$	$Y'_{\delta\delta v} = 1242.8$	$N'_{\delta\delta v} = -526.8$
$X'_0 = 0$	$Y'_{vv\delta} = 17722.4$	$N'_{vv\delta} = -6223.0$
	$Y'_{vvr} = 20234.0$	$N'_{vvr} = -13552.0$
	$Y'_{vvv} = -58135.2$	$N'_{vvv} = 2430.6$
	$Y'_0 = 0$	$N'_0 = 0$

Table 3
Dimensional quantities and corresponding non-dimensioning factors for the fishing vessel simulated by Abkowitz Model.

	Non − dimensioning factor
X, *Y*	$\frac{1}{2}\rho L^2U^2$
N	$\frac{1}{2}\rho L^3U^2$
I_{zz}	$\frac{1}{2}\rho L^5$
m	$\frac{1}{2}\rho L^3$
u, *v*	*U*
r	*U*/*L*

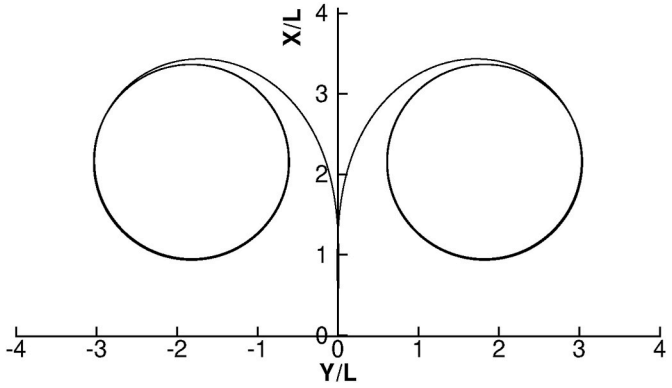

Fig. 5. Turning test for fishing vessel (± 35 deg.).

Table 4
Turning test parameters as computed by different approaches for fishing vessel.

	Obreja etal.	*Tribon code*	*Present code*
Advance/Ship Length	3.44	4.11	3.31
Transfer/Ship Length	1.39	1.88	1.49
Tactical Diameter/Ship Length	3.04	3.93	3.03
Steady Diameter/Ship Length	3.02	3.09	2.49
Speed Loss	59%	63%	60%

4.1. Determination of transfer function

The transfer function representing the behaviour of a system to a given input is required for the operation of a controller. A frequently used, simple but accurate transfer function for the rudder control of a ship is the first-order Nomoto model (Nomoto et al., 1957) which is defined as

$$\frac{r}{\delta}(s) = \frac{K}{(1+T\,s)} \tag{14}$$

where K the so-called Nomoto gain constant, T the time constant, and δ the rudder angle, $r = \dot{\psi}$ as defined before. In terms of the heading angle ψ, equation (14) becomes (Moreira et al., 2005)

$$\frac{\psi}{\delta}(s) = \frac{K(1+T_3 s)}{s(1+T_1 s)(1+T_2 s)} \approx \frac{K}{s(1+T\,s)} \tag{15}$$

To be able to use the transfer function the constants must be determined for the ship considered. Clarke (2003) related the zigzag manoeuvres of a ship to the first-order Nomoto transfer function so that K and T could be calculated from the actual zigzag manoeuvre tests or numerical simulations. Accordingly, K is calculated from $K = -(\psi_1 - \psi_2)/\int_{t_1}^{t_2}\delta dt$, where ψ_1 and ψ_2 are the first and second heading overshoot angles and t_1 and t_2 are the corresponding instants of the 20 − 20 zigzag manoeuvre. $\int_{t_1}^{t_2}\delta dt$ is the total area under rudder command within the given time interval. the 20 − 20 zigzag test simulation. Strictly speaking the actual instantaneous rudder angles should be used for computing the shaded area; but here, as a good approximation, the idealized rudder commands, which are taken to be identical with the actual rudder

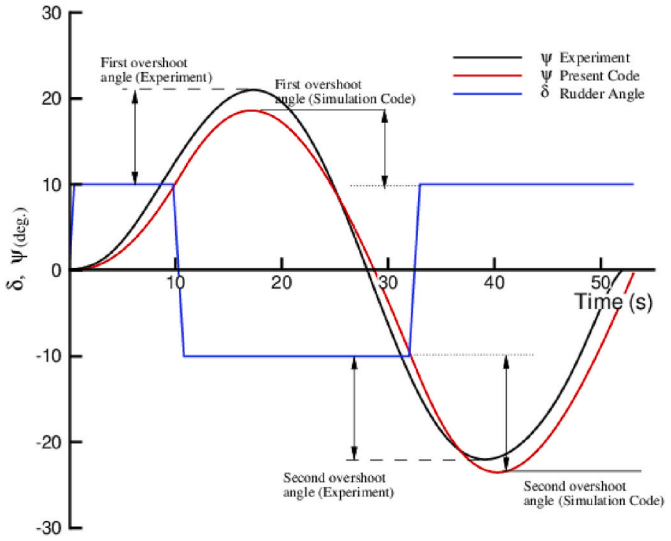

Fig. 6. Zigzag manoeuvre by applying ±10° rudder angles for fishing vessel. Experimental measurement (black line), present simulation (red line), rudder angle (blue line). (For interpretation of the references to colour in this figure legend, the reader is referred to the Web version of this article.)

Table 5
Main characteristics of KVLCC2 tanker.

L_{PP}	320.0 m
B	58.0 m
T	20.8 m
▽	312,600 m^3
C_B	0.81
$k_{zz}(0.25Lpp)$	80.0 m
X_G	11.2 m
V	7.9732 m/s
D	9.86 m
H	15.8 m
A	112.5 m^2

Table 6
Hydrodynamic coefficients of KVLCC2 tanker.

$m_x' = 0.022$	$m_y' = 0.223$	$J_{zz}' = 0.011$
$X_{rr}' = 0.011$	$Y_r' = 0.083$	$N_r' = -0.049$
$X_{vr}' = 0.002$	$Y_v' = -0.315$	$N_v' = -0.137$
$X_{vv}' = -0.04$	$Y_{vrr}' = -0.391$	$N_{vrr}' = 0.055$
$X_{vvvv}' = 0.771$	$Y_{vvr}' = 0.379$	$N_{vvr}' = -0.294$
$X_0' = -0.022$	$Y_{vvv}' = 1242.8$	$N_{vvv}' = -0.03$
$\delta_\star = 2.34$	$Y_{rrr}' = 0.008$	$N_{rrr}' = -0.013$
$a_H = 0.312$	$x_R' = -0.5$	$x_P = -0.48$
$x_H' = -0.464$	$w_{P0} = 0.35$	$t_R = 0.387$
$t = 0.22$	$\ell' = -0.71$	$\lambda = 1.827$
$\kappa = 0.5$	$\varepsilon = 1.09$	$n = 1.53$
$\gamma^+ = 0.64$	$\gamma^- = 0.395$	

Table 7
Dimensional quantities and corresponding non-dimensioning factors for the KVLCC2 tanker simulated by MMG Model.

	Non − dimensionalized by
X, Y	$\frac{1}{2}\rho LdU^2$
N	$\frac{1}{2}\rho L^2dU^2$
I_{zz}	$\frac{1}{2}\rho L^4d$
m	$\frac{1}{2}\rho L^2d$
u, v	*U*
r	*U/L*

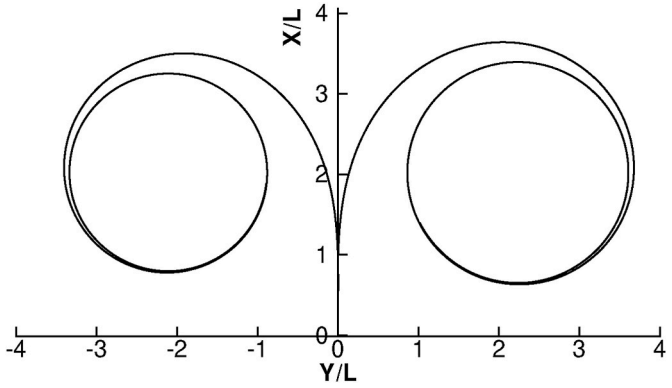

Fig. 7. Turning test for KVLCC2 tanker (± 35 deg.).

Table 8
Turning test parameters as computed by different approaches for KVLCC2 tanker.

		MARIN	*Yasukawa*	*Sukas*	*Present*
		FR	*& Yoshimura*	*et al.*	*code*
Ad./ L_{pp}		3.25	3.62	3.10	3.64
Tr./ L_{pp}	(+ 35°)	1.36	1.58	1.35	1.56
TD/ L_{pp}		3.34	3.71	3.16	3.68
Ad./ L_{pp}		3.11	3.56	3.10	3.50
Tr./ L_{pp}	(− 35°)	−1.22	−1.51	−1.23	−1.43
TD/ L_{pp}		−3.08	−3.59	−2.90	−3.41

angles, are used to compute this area. Once K is calculated, T is obtained from $K/T = -(r_3 - r_4)/\int_{t_3}^{t_4}\delta dt$, where r_3 and r_4 are the angular velocities of heading at the zero heading angles with t_3 and t_4 being the corresponding times. For the fishing vessel *Città di Genova* considered in §3.1, using the 20 − 20 zigzag manoeuvring simulation at $U = 10$ knots give $K = 0.184\,s^{-1}$ and $T = 6.816$ s as the constants of the first-order Nomoto model.

Simulations presented in §5.2 had first been carried out by employing the Nomoto model which gave quite acceptable results. Nevertheless, a more practical and accurate way of obtaining the transfer function is possible. Inclusion of non-linear effects and better performance for high frequencies (large perturbations requiring frequent adjustments) are achieved by a transfer function that can be obtained from MATLAB function LINMOD. Again, using the zigzag test validated in §3.1 for the fishing vessel *Citta di Genova*, the open-loop transfer function is obtained as follows.

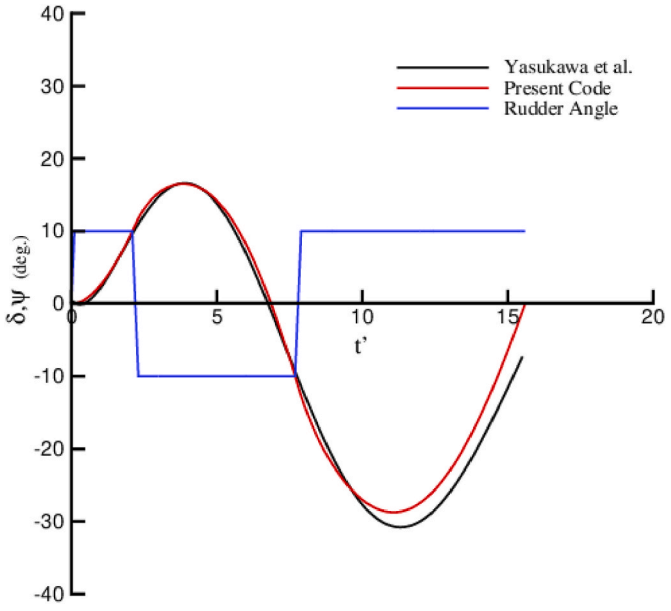

Fig. 8. Zigzag manoeuvre by applying ±10° rudder angles for KVLCC2 tanker. Yasukawa et al. (Yasukawa and Yoshimura, 2015) (black line), present simulation (red line), rudder angle (blue line). (For interpretation of the references to colour in this figure legend, the reader is referred to the Web version of this article.)

$$\frac{\psi}{\delta}(s) = G(s) = \frac{0.01666s + 0.00793}{s^3 + 0.2548s^2 + 0.02366s} \tag{16}$$

The above transfer function $G(s)$ is used in the simulations presented in §5.2. Equation (16) is observed to perform better than the Nomoto transfer function (15), which is validated only for constant heading and ship speed (Skjetne, 2003).

The corresponding closed-loop system shown in Fig. 9 has the transfer function,

$$\frac{C(s)}{R(s)} = \frac{G(s)}{1 + G(s)H(s)} \tag{17}$$

where $C(s)$ is the output (heading angle) and $R(s)$ the input (rudder angle), $G(s)$ the open-loop transfer function given by (16), $H(s)$ the feedback transfer function which is taken as $H(s) = 1$ in the present Simulink code. Applying the Routh-Hurwitz stability criterium to the closed-loop system reveals that the system is stable hence controllable.

An uncertainty analysis considering the effects of variations in disturbance signals, specifically external forces for the present case, and system parameters that define the transfer function, would be desirable. However, such an analysis is a separate work in itself, usually subject of an individual study, hence exceeds the limits of present work.

4.2. Determination of rudder angle

A PD controller, as indicated above, has a proportional and a de-

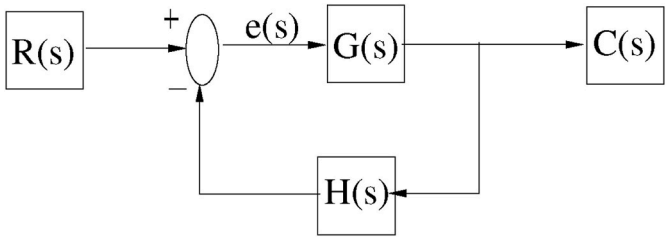

Fig. 9. Block diagram for the closed-loop system for the ship.

rivative control. Denoting $e(t)$ as the error between the desired heading angle ψ_d and the instantaneous heading angle ψ, the rudder angle is computed from

$$\delta(t) = K_p e(t) + K_d \frac{de(t)}{dt} \tag{18}$$

where K_p and K_d are the proportional and derivative control constants with numerical values of 1.52 and 17.29 respectively for the present simulations.

The desired heading angle is computed according to the instantaneous ship position (x_{sp}, y_{sp}) and the destination point (x_{dp}, y_{dp})

$$\psi_d = \arctan\left(\frac{y_{dp} - y_{sp}}{x_{dp} - x_{sp}}\right) \tag{19}$$

Since the heading angle ψ is known at every step of simulation and ψ_d is calculated from (19), the error $e(t) = \psi_d - \psi$ can be determined and used in equation (18) to obtain δ at each time step. Fig. 10 shows the block diagram for the rudder angle determination with PD and fuzzy-like PD controls.

5. Autopiloting across a narrow strait with currents

The Strait of Istanbul, or the Bosphorus, is among the few narrow sea passages in the World with challenging currents. Every day hundreds of passenger boats, ferries, yachts, ships, tankers roam about in the strait, crossing and re-crossing between the European and Asian sides of Istanbul or between the Sea of Marmara and Black Sea. A photograph of the Bosphorus taken from Üsküdar at the Asian side with the view of Beşiktaş across the strait at the European side is given in Fig. 11.

Busy sea traffic especially between the continents offers readily accessible and interesting observation possibilities of the routes followed by ships. To this end, field observations and records of routes of passenger boats frequently crossing the Bosphorus between Beşiktaş (European side) and Üsküdar (Asian side) were planned. The aim of these actual field observations was to determine the paths followed by captains to steer their vessels to a nearby destination point under the disturbing effect of a more or less steady unidirectional current. Once these routes have been determined they could be compared with autopiloted simulations of a similar vessel for the same case. This part of the present work precisely carries out such a plan.

5.1. Recordings of routes of a passenger boat crossing bosphorus

The Strait of Istanbul has a two-layer flow regime with the upper layer flowing from the Black Sea towards the Sea of Marmara and the lower layer in the opposite direction. The upper layer flow is termed barotropic as it is forced by the pressure difference arising from water level difference at either ends of the channel. On the other hand, the lower-layer flow is termed baroclinic and essentially is a result of the density difference between two layers. Although the upper layer flow is occasionally *blocked* due to strong opposing winds the usual two-layer flow regime is maintained most of the time. The current velocity in the upper-layer, basically in the south-west direction, varies between 1 to 2 knots (˜0.5 – 1 m/s) but may occasionally reach 4 knots (˜2 m/s) and even more (Beji et al., 2018).

Fig. 11. A snapshot viewing Beşiktaş (European Continent) from Üsküdar (Asian Continent) with a typical passenger boat crossing in between.

On February 25, 2020 a field survey was conducted by recording the routes of a relatively small passenger boat of 37 m-length for three round trips across the Strait of Istanbul between Beşiktaş (Europena side) and Üsküdar (Asian side). During the survey the sea was a bit choppy, as could be noted from Fig. 11, which also shows the boat travelled, but otherwise made no appreciable effect on vessels. The current speed was put within the range 1 – 2 knots by the boat captain. In total six crossings were done, three from the European side to Asian side and three in the opposite direction. Instantaneous co-ordinates of the boat trip were continuously recorded in time via a mobile phone application of Google. Fig. 12 shows two of the routes recorded while travelling from Beşiktaş to Üsküdar. During one of these crossings a tanker making her way to the Black Sea obstructed the passage of the passenger boat and forced her to make a substantial detour; therefore, this particular recording of the path has been excluded from Fig. 12. The recorded routes from Üsküdar to Beşiktaş are shown in Fig. 13.

The prominent feature of the recorded paths is their arch-like appearance. Considering that the current direction is from left to right in the figures, reason for bending of the paths to either sides may be questioned. The answer lies with the initial heading of the boat, which is dictated by the sea traffic at the time. Thus, if the captain is forced to head against current at the start then the entire path becomes a curve

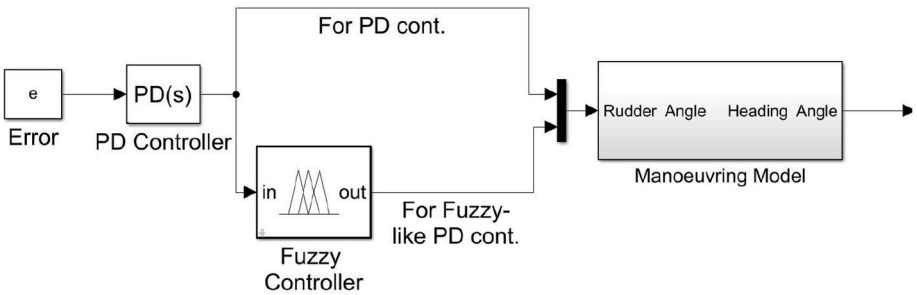

Fig. 10. Block diagram for rudder control.

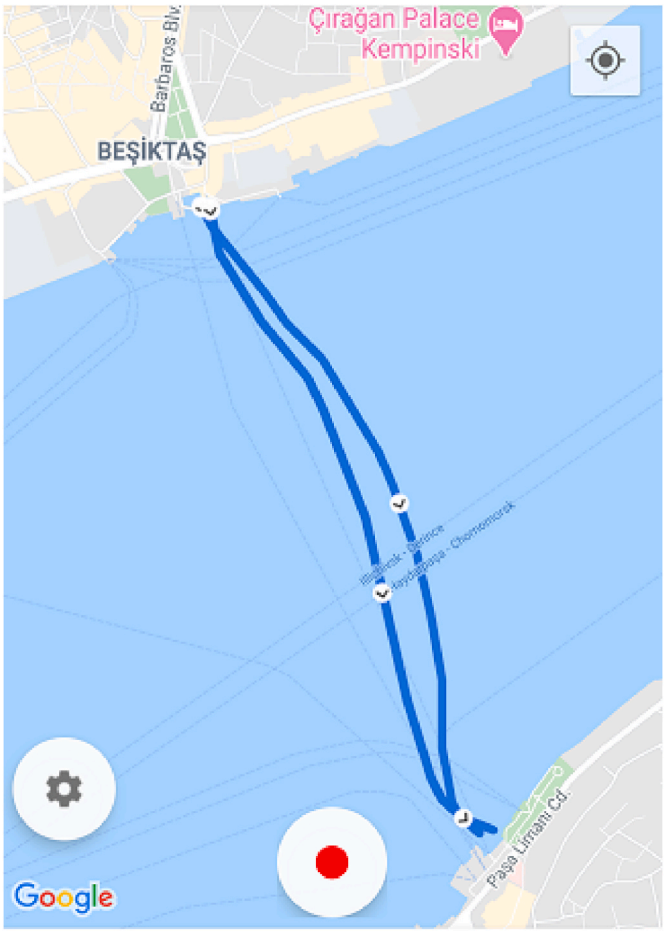

Fig. 12. Passenger boat paths recorded during trips from Beşiktaş to Üsküdar.

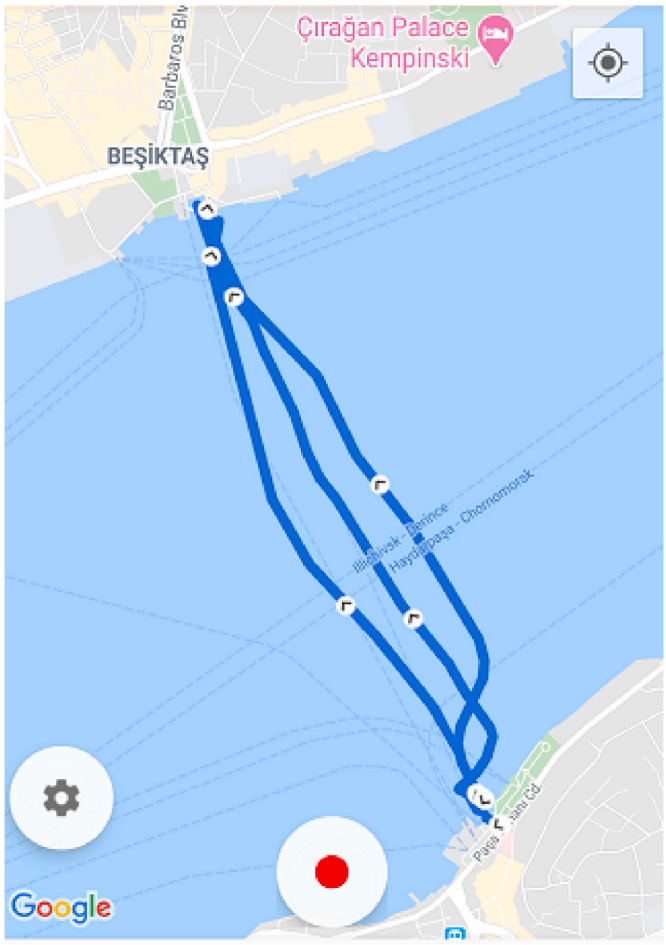

Fig. 13. Passenger boat paths recorded during trips from Üsküdar to Beşiktaş.

bent in the direction of current; otherwise, the bent is in the opposite direction. This particular feature also confirms the symmetrical nature of the problem. When crossing a channel with a uniform current perpendicular to the travel direction to reach a destination directly ahead it is equally plausible to follow one of the two choices. First, the initial heading of the boat can be against the current at an angle with the target so that deviation from the straight path becomes maximum in the middle of the channel. The boat then shifts her heading away from the current back towards the target. Second, the initial heading of the boat can be in the direction of the current and not against it. Thus, the boat follows a path which is a mirror image of the first path about the line connecting departure and arrival points. In the first case then the boats fights against the current halfway of the route and then goes with it; in the second case the boat goes halfway with the current and then fights against it.

5.2. Controlled simulations of a vessel crossing bosphorus

Controlled simulations of a vessel travelling under conditions similar to those of the Bosphorus are now presented for different current speeds. PD and fuzzy-like PD controllers are used separately by coupling each one with the present numerical manoeuvring code.

In terms of general characteristics, the fishing vessel *Città di Genova* tested in §3.1 is considered reasonably well comparable with a typical passenger boat operating in the Bosphorus. Thus, knowing all the hydrodynamic properties for manoeuvring and having already obtained in §4.1 the transfer function from MATLAB-LINMOD, the autopiloted simulations of this particular vessel can be carried out. According to the case scenario the vessel is to travel from Üsküdar to Beşiktaş at constant velocity $u = 10$ knots, in line with the speed of the boat travelled in field survey. The current velocity is assumed uniform across the Strait of Istanbul and the simulations are done for three different current velocities; namely, $V_c = 1$, 1.5, and 2 knots. Since two different controllers, PD and fuzzy-like PD, are employed, six different simulations are carried out. Fig. 14 shows the changes in the rudder angle during each trip for PD and fuzzy-like PD controllers for three different current speeds.

Figs. 15–17 show the simulations for $V_c = 1$, 1.5, and 2 knots. Red and blue lines trace the paths taken under PD and fuzzy-like PD controls, respectively. As the ship begins its trip parallel to the channel with a heading angle 90° to the target direction, fuzzy-like PD makes sharper adjustments compared to the PD alone but as the ship more or less settles to its route around $t = 10$ s the control of fuzzy-like PD becomes smoother.

Table 9 presents certain quantities obtained from simulations for different current velocities in order to compare the performances of PD and fuzzy-PD controllers. In the table, t denotes the duration of travel from the departure point to the destination in seconds, X is the distance to the target straight ahead of the vessel, and Y is the sideways deviation distance from the target at the arrival point. This deviation is zero if the vessel is precisely at the terminal point.

Like Figs. 15–17, Table 9 reveals definitely better performance for the fuzzy-like PD in terms of both the travel duration and the proximity of terminal point of simulation to the targeted location. Nevertheless, the routes dictated by both the PD and the fuzzy-like PD controller are within the paths taken by human piloting shown in Figs. 12 and 13. The maximum deviation for human piloting is around 135 m for approximately $V_c = 1.5$ knots, as estimated by the boat captain. The corresponding autopiloted trip has around 32 m of maximum deviation for

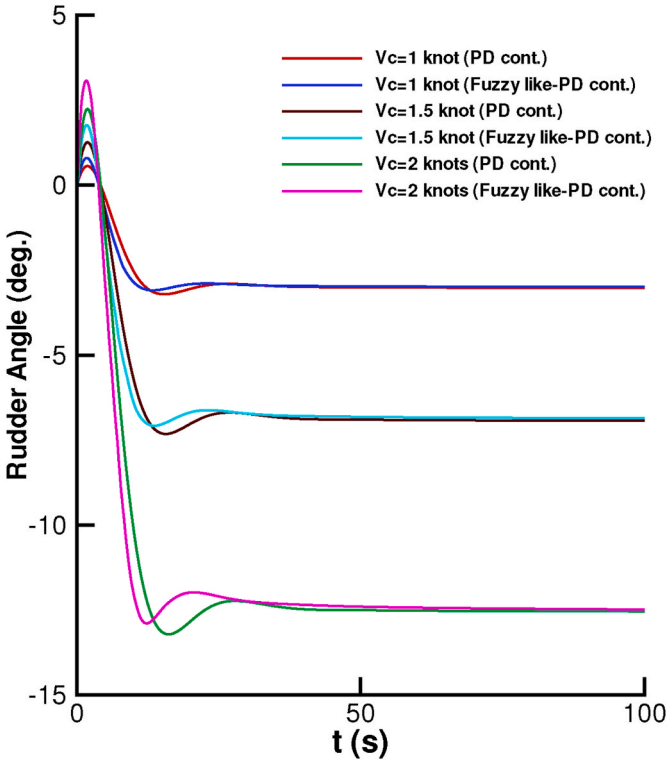

Fig. 14. Change of rudder angle during the simulation under different current velocities for PD and fuzzy-like PD controllers.

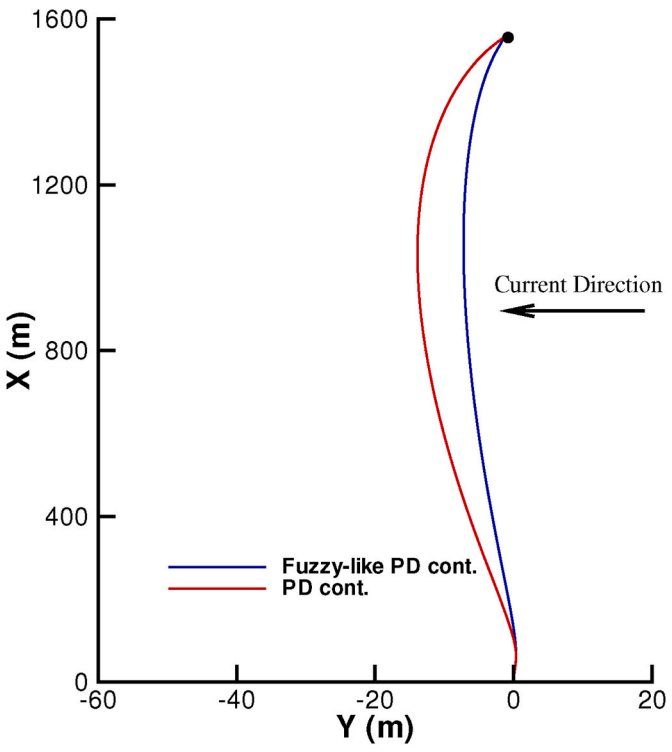

Fig. 15. Controlled simulations of fishing vessel crossing Bosphorus using PD and fuzzy-PD controllers for current speed $V_c = 1$ knot.

the PD controller and the fuzzy-like PD is less than 20 m. We must however be fair in our judgement of the human piloting and indicate that the greater part of the deviations from the route is caused by the sea traffic present as observed during trips.

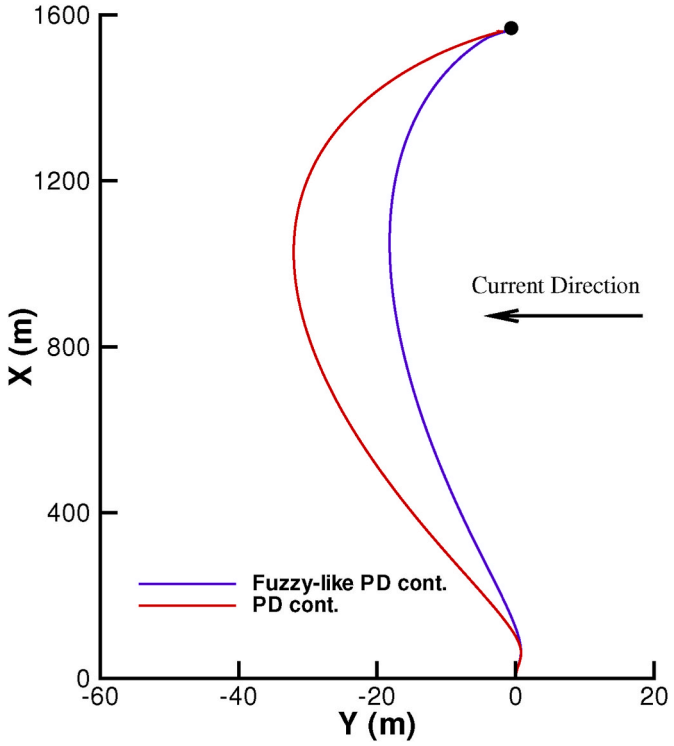

Fig. 16. Controlled simulations of fishing vessel crossing Bosphorus using PD and fuzzy-PD controllers for current speed $V_c = 1.5$ knots.

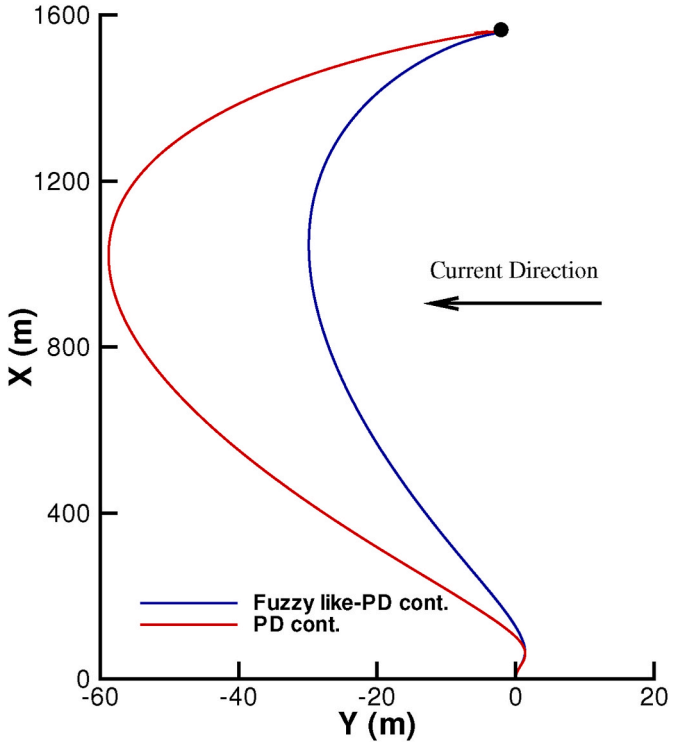

Fig. 17. Controlled simulations of fishing vessel crossing Bosphorus using PD and fuzzy-PD controllers for current speed $V_c = 2$ knots.

6. Concluding remarks

A Simulink code has been created for the numerical solution of manoeuvring equations of a surface vessel. The code offers both the

Table 9
Simulation results for PD and fuzzy-like PD controllers.

		V_c = 1 kn.	V_c = 1.5 kn.	V_c = 2 kn.
PD	*t*	303.3 s	303.6 s	304.5 s
	X	1560.0 m	1560.0 m	1560.0 m
	Y	−1.0 m	−1.9 m	−3.0 m
Fuzzy −	*t*	303.2 s	303.3 s	303.5 s
like	*X*	1560.0 m	1560.0 m	1560.0 m
PD	*Y*	−1.1 m	−1.5 m	−1.6 m

Abkowitz and MMG model as options to the user so that according to the available data for the vessel considered the appropriate model can be selected. Benchmarks tests for two different ships have been carried out by the use of Abkowitz and MMG model, separately. Comparisons of test results with other sources give confidence for the code developed.

Real time records of the position of a passenger boat crossing the Strait of Istanbul have been taken via a mobile application of Google. Autopilot simulations for a similar vessel guided by the PD and fuzzy-like PD controls operating with the Simulink code have been carried out. The heading hence the route is determined by controlling the rudder angle at each time step according to the current status of the ship in relation to the destination. In comparison with PD controller, paths dictated by the fuzzy-like PD controller define relatively less deviated shorter routes.

In closing, research works such as the present one can be expected to lay the general framework upon which more sophisticated and detailed actual control systems can be built.

CRediT authorship contribution statement

G. Budak: Responsible for methodology, carrying out the work, software, field observations and measurements, writing, reviewing, and editing. **S. Beji:** Responsible for conceptualization, supervising, and final writing, reviewing, and editing.

Declaration of competing interest

The authors declare that they have no known competing financial interests or personal relationships that could have appeared to influence the work reported in this paper.

Acknowledgements

Steadfast efforts of the Editor-in-Chief and Deputy Editor are gratefully acknowledged in handling the review process smoothly in these trying times. The authors sincerely thank two anonymous referees whose constructive comments and suggestions have improved the presentation and contents of this work greatly.

References

Aksu, E., Köse, E., 2017. Evaluation of mathematical models for tankers' maneuvering motions. Journal of ETA Maritime Science, JEMS 5 (1), 95–109.
Beji, S., Erdik, T., 2018. Hydrodynamics and modelling of Turkish straits. Turkish Marine Research Foundation (TUDAV), Publication No: 47 Istanbul. In: Ünlü, S., Alpar, B., Öztürk, B. (Eds.), Oil Spill along the Turkish Straits Sea Area: Accidents, Environmental Pollution, Socio-Economic Impacts and Protection, pp. 79–90. Turkey.
Bhattacharya, S.K., Rajesh, G., Gupta, D.K., 2011. Fuzzy autopilot for ship maneuvering. Int. Shipbuild. Prog. 191–218.
Cimen, T., Banks, P.B., 2004. Nonlinear Optimal Tracking Control with Application to Super-tankers for Autopilot Design. Automatica, pp. 1845–1863.
Clarke, D., 2003. The foundations of steering and manoeuvring. In: Proceedings of 6th Conference on Maneuvring and Control of Marine Crafts (MCMC), vol.2–16.
Comstock, J.P., 1986. Principles of Naval Architecture. The Society of Naval Architects and Marine Engineers, New York, N. Y.
Fang, M., Lin, Y., 2015. The optimization of ship weather-routing algorithm based on the composite influence of multi-dynamic elements (ii): optimized routings. Appl. Ocean Res. 50, 130–140.
Feng, Y.X., X-K, Z., 2018. Ship course keeping control based on nonlinear decoration fuzzy pid. Ship Eng 40, 202–205.
Fossen, T.I., 2011. Handbook of Marine Craft Hydrodynamics and Motion Control. John Wiley & Sons Ltd., West Sussex, United Kingdom.
Hirdaris, S., Bai, W., Dessi, D., Ergin, A., Gu, X., Hermundstad, O., Huijsmans, R., Iijima, K., Nielsen, U., Parunov, J., Fonseca, N., Papanikolaou, A., Argyriadis, K., Incecik, A., 2014. Loads for use in the design of ships and offshore structures. Ocean Eng. 78, 131–174.
Johnson, M.A., Moradi, H.M.E., 2005. PID Control New Identification and Design Methods. Springer-Verlag, London.
Källström, C., Eriksson, J., Aström, K.J., Sten, L., Thorell, N.E., 1977. Adaptive Autopilots for Steering of Large Tankers. Department of Automatic Control, Lund Institute of Technology (LTH). Technical Report.
Kim, M., Hizir, O., Turan, O., Incecik, A., 2017. Numerical studies on added resistance and motions of kvlcc2 in head seas for various ship speeds. Ocean Eng. 140, 466–476.
Kurowski, M., Köckritz, O., Korte, H., 2013. Full-state maneuvre planning system for marine vehicles. 9th IFAC Conference on Control Applications in Marine Systems, pp. 17–20.
Le, M., N, S.H., N, L.A., 2004. Study on a new and effective fuzzy pid ship autopilot. Artif. Life Robot. 8, 197–201.
Moreira, L., Fossen, T.I., Soares, C.G., 2005. Modeling, guidance and control of "Esso Osaka" model. Norwegian University of Science and Technology, Throndheim. Technical Report.
Moreira, L., Fossen, T.I., Soares, C.G., 2007. Path following control system for a tanker ship model. Ocean Eng. 34, 2074–2085.
Nomoto, K., Taguchi, T., Honda, K., Hirano, S., 1957. On the Steering Qualities of Ships.
Obreja, D., Nabergoj, R., Crudu, L., Pacuraru-Popoiu, S., 2010. Identification of hydrodynamic coefficients for manoeuvring simulation model of a fishing vessel. Ocean Eng. 37, 678–687.
Ogawa, A., Kasai, H., 1978. On the mathematical model of manoeuvring motion of ships. Int. Shipbuild. Prog. 25 (292), 306–319.
Perez, T., Smogeli, O.N., Fossen, T.I., Sorensen, A.J., 2006. An overview of marine systems simulator: Simulink toolbox for marine control systems. Model. Ident. Contr. 27, 259–275.
Seo, Y., Kim, S., 2011. Numerical analysis on ship maneuvering coupled with ship motion in waves. Ocean Eng. 38, 1934–1945.
SIMMAN, 2008. Part c: captive and free model test data. workshop on verification and validation of ship manoeuvring simulation methods. In: Workshop Proceedings, vol. 1. Copenhagen.
Skjetne, R., 2003. Ship Maneuvering: the Past, the Present and the Future. Sea Technology.
Sukas, O.F., Kinaci, O.K., Bal, S., 2019a. System-based prediction of maneuvering performance of twin-propeller and twin-rudder ship using a modular mathematical model. Appl. Ocean Res. 84, 145–162.
Sukas, O.F., Kinaci, O.K., Bal, S., 2019b. Theoretical background and application of mansim for ship maneuvering simulations. Ocean Eng. 192, 106239.
Tahara, Y., Tohyama, S., Katsui, T., 2006. Cfd-based multi-objective optimization method for ship design. Int. J. Numer. Methods Fluid. 52, 499–527.
Tezdogan, T., Demirel, Y.K., Kellett, P., Khorasanchi, M., Incecik, A., Turan, O., 2015. Full-scale unsteady rans cfd simulations of ship behaviour and performance in head seas due to slow steaming. Ocean Eng. 97, 186–206.
Xia, Y., Zheng, S., Yang, Y., Qu, Z., 2018. Ship maneuvering performance prediction based on mmg model. IOP Conf. Ser. Mater. Sci. Eng. 452, 042046.
Yasukawa, H., Yoshimura, Y., 2015. Introduction of mmg standard method for ship maneuvering predictions. J. Mar. Sci. Technol. 20, 37–52.
Yoshimura, Y., 2005. Mathematical Model for Manoeuvring Ship Motion (Mmg Model). Tokyo. In: Workshop on Mathematical Models for Operations Involving Ship-Ship Interaction.